Journal of Biomedical Optics

SPIEDigitalLibrary.org/jbo

Using optical profilometry to characterize cell membrane roughness influenced by amyloid-beta 42 aggregates and electric fields

Huei-Jyuan Pan
Ruei-Lin Wang
Jian-Long Xiao
Yu-Jen Chang
Ji-Yen Cheng
Yun-Ru Chen
Chau-Hwang Lee

SPIE

Using optical profilometry to characterize cell membrane roughness influenced by amyloid-beta 42 aggregates and electric fields

Huei-Jyuan Pan,[a] Ruei-Lin Wang,[b,c] Jian-Long Xiao,[a] Yu-Jen Chang,[d] Ji-Yen Cheng,[a,b,c,e] Yun-Ru Chen,[d] and Chau-Hwang Lee[a,b,c]
[a]Research Center for Applied Sciences, Academia Sinica, Taipei 11529, Taiwan
[b]National Yang-Ming University, Institute of Biophotonics, Taipei 11221, Taiwan
[c]National Yang-Ming University, Biophotonics and Molecular Imaging Research Center (BMIRC), Taipei 11221, Taiwan
[d]Genomics Research Center, Academia Sinica, Taipei 11529, Taiwan
[e]National Taiwan Ocean University, Department of Mechanical and Mechatronic Engineering, Keelung 20224, Taiwan

Abstract. The membrane roughness of Neuro-2a neroblastoma cells is measured by using noninterferometric wide-field optical profilometry. The cells are treated with the fibril and oligomer conformers of amyloid-beta (Aβ) 42, which is a peptide of 42 amino acids related to the development of Alzheimer's disease. We find that both the Aβ42 fibrils and Aβ42 oligomers reduced the cell membrane roughness, but the effect of Aβ42 oligomers was faster and stronger than that of the fibrils. We also apply direct-current electric field (dcEF) stimulations on the cells. A dcEF of 300 mV/mm can increase the membrane roughness under the treatment of Aβ42. These results suggest that Aβ42 can decrease the membrane compliance of live neuroblastoma cells, and dcEFs may counteract this effect. [DOI: 10.1117/1.JBO.19.1.011009]

Keywords: membrane roughness; amyloid-beta 42; electric field; NIWOP.

Paper 130151SSRR received Mar. 18, 2013; revised manuscript received Jun. 21, 2013; accepted for publication Jun. 27, 2013; published online Jul. 26, 2013.

1 Introduction

Alzheimer's disease (AD) is a progressive neurodegenerative disease in which one of the defining characteristics is global cognitive decline including memory,[1] orientation, judgment, and reasoning. Amyloid-beta 42 (Aβ42) is a peptide composed of 42 amino acids that is believed to be related to the development of AD.[2] Aβ peptides can bind to various biomolecules, such as proteins, lipids, and proteoglycans, and therefore cause toxic effects to neurons by perturbing the properties and functions of plasma membranes.[3–5] The Aβ peptides can assemble into various degrees of polymerization, and the conformations of oligomers, proto-fibrils, and fibrils are found to exist in brain lesions of AD patients. Both Aβ fibrils and oligomers are demonstrated to be neurotoxic. Aβ oligomers are also shown to correlate with cognitive impairment and induce synaptic dysfunction,[6] apoptosis, and mouse abnormal behaviors.[7] It has been verified that the membrane stiffness of Neuro-2a (N2a) neuroblastoma cells is increased by Aβ oligomers.[8] In addition, Aβ pore-like oligomers and Aβ channels have been observed on lipid bilayers.[9] Therefore, we may conjecture that the Aβ peptides have the ability to vary other mechanical characteristics of cell membranes.

Recently, a number of groups have demonstrated that the stimulation of electrical fields (EFs) on neuronal cells can affect specific cell behaviors, including migration directions,[10] cell orientation,[11] growth of neurites,[12,13] and neuron–neuron contact.[14] Owing to the nonintrusive nature of the EF stimulation on live cells, EFs are believed to be developed into potential therapeutic applications for a variety of neurological diseases. Because both the EF and Aβ peptides show evident variations on neuronal cells, it is intriguing to know how cells respond to these two external stimulations simultaneously.

In the present work, we used the noninterferometric wide-field optical profilometry (NIWOP) technique to measure the membrane roughness of N2a cells under both the treatments of Aβ42 peptides and EFs. The NIWOP technique has been used to measure the dynamical membrane ripples on live cells.[15–17] Compared with atomic force microscopy, the NIWOP technique is faster and noncontact, and therefore the membrane topography as well as the cell viability is not perturbed during the measurement. In addition, because the NIWOP setup is constructed on a conventional optical microscope, it is compatible with current cell culture devices and easy to conduct various treatments during the observation.

2 Materials and Methods

2.1 *Cell Culture Device Capable of Conducting EF Stimulations*

We remodeled an ordinary 100-mm culture dish for the EF stimulation according to the design described by McCaig et al.[18] Figure 1 shows the layout and a photograph of this culture device. The volume of the cell chamber is $44.5 \times 2.5 \times 0.063$ mm^3. We did not coat any cell-adhesive proteins or molecules on the bottom of the culture dish. The acrylic sheets and double-sided tapes (PET8018, 3M Corp., St. Paul, MN, USA) were incised by a CO_2 laser cutting machine. The EF was built

Address all correspondence to: Chau-Hwang Lee, National Yang-Ming University, Institute of Biophotonics, 155 Sec. 2, Li-Nong Street, Taipei 11221, Taiwan. Tel: +886-2-28267245; Fax: +886-2-28235460; E-mail: chlee4@ym.edu.tw

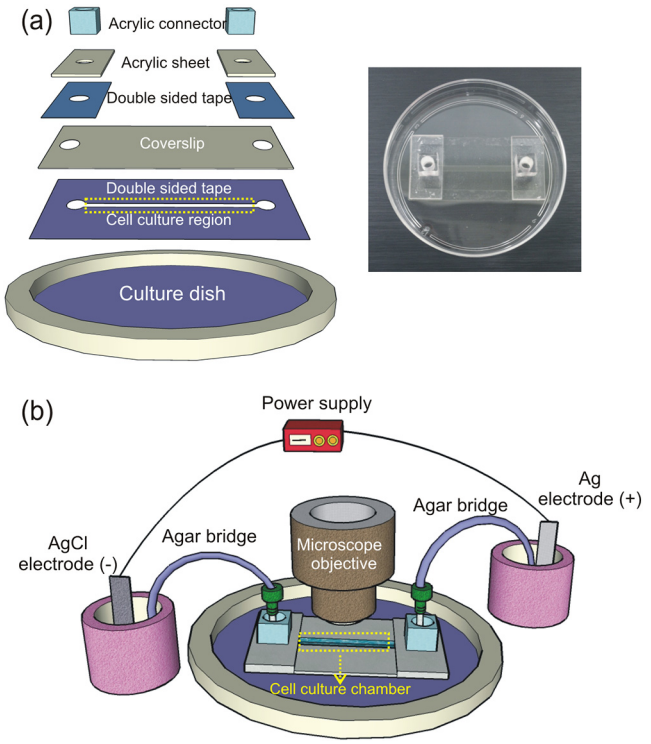

Fig. 1 (a) A schematic diagram and a photograph of the culture device for the electrical field (EF) stimulation and noninterferometric wide-field optical profilometry (NIWOP) observation. (b) Setup for the EF treatment and optical observation on live cells.

through two agar bridges connecting the culture device and two bottles of phosphate-buffered saline (PBS). The anode was a silver (Ag) electrode, and the cathode was a AgCl electrode. When the direct-current (dc) power supply was turned on, the Cl^- ions in the cell culture medium were forced to move toward the anode and thus an ion current was formed. Because the resistance in the culture chamber was finite, the ion current produced a potential difference along the direction of the ion movement. Because the ion current was increased as the applied voltage, we could have an EF strength inside the cell culture region proportional to the voltage. The EFs were calculated as the potential difference divided by the distance between the two measuring probes inserted into the cell culture region. We tested eight devices with an applied voltage up to 25 V. A direct-current electric field (dcEF) strength as high as 500 mV/mm could be built in these culture devices and the EF strength was linear with the applied voltage (data not shown). In the following experiments, we fixed the strength of EF at 300 mV/mm because this EF strength led to obvious variations in membrane roughness and showed no degradation on cell viability.

2.2 *Setup of NIWOP*

Figure 2 shows the setup of the NIWOP system. The NIWOP technique is based on differential confocal microscopy and wide-field optical sectioning microscopy.[19] In short, we used the structured-illumination wide-field sectioning microscopy[20] to obtain an intensity axial response curve similar to that of confocal microscopy. Then we placed the cell dorsal surface into the linear region of this axial response curve; in this region the intensity is linearly proportional to the height of the sample. Therefore, we can obtain the heights of cell membranes after a calibration process.[15] The height measurement dynamic

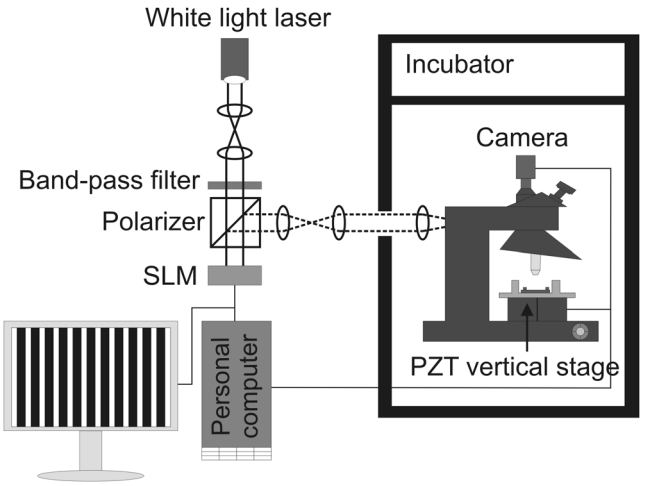

Fig. 2 A schematic diagram of the setup of NIWOP. SLM, spatial light modulator; PZT, piezo-electric transducer.

range is determined by the width of the intensity axial response curve, which is set by the numerical aperture of the objective and the period of the projected illumination pattern.[19] The accuracy of height detection is limited by signal fluctuation divided by the slope of the linear region of this axial response curve. In the structured-illumination wide-field sectioning microscopy, three images (I_1, I_2, I_3) with the illumination pattern shifted by one third of the pattern period are captured and processed with the square-law detection principle:

$$I_s = \sqrt{(I_1 - I_2)^2 + (I_2 - I_3)^2 + (I_1 - I_3)^2}.$$

Therefore the imaging speed is lower than that of conventional wide-field imaging. In the present work, the image acquisition rate of the NIWOP system was 12 images/min (equivalent to 36 frames/min). With a 40× NA 0.80 objective lens the depth accuracy is ~52 nm, and the measurement dynamic range is ~3000 nm. Other details of NIWOP measurement on cell membrane roughness can be found in our previous publications.[15–17] The NIWOP system was constructed on an upright microscope, and we used a spatial light modulator to generate the pattern for structured illumination. The microscope and the piezo-electric transducer (PZT)-driven vertical stage were placed in a temperature-controlled incubator, which kept the temperature at 37 ± 1°C during the experiment.

2.3 *Cell Culture and Aβ42 preparation*

The cells we used in the present work were from a mouse neuroblastoma cell line N2a. The culture medium was minimum essential medium alpha (12571, Gibco, Life Technologies, NY, USA) with 10% fetal bovine serum (FBS) and 1% antibiotic pen-strep-ampho. Before the experiments, we used 10 μM retinoic acid (R2625, Sigma-Aldrich, St. Louis, MO, USA) and reduced the concentration of FBS to 1% to differentiate the cells for neurite growth.

To prepare Aβ42 oligomers and fibrils, we used the following procedures that were modified from the protocols proposed by Dahlgren et al.[21] The Aβ peptide was first dissolved by hexafluoroisopropanol (HFIP) in 2.5 mg/mL to dissociate Aβ preaggregates. HFIP was evaporated in vacuum for >3 h and Aβ films were dissolved in anhydrous dimethyl sulfoxide (DMSO). For Aβ oligomers preparation, Aβ stock in DMSO at 5 mM was

refolded in Dulbecco's modified Eagle medium/nutrient mixture medium (21041, Gibco, Life Technologies, NY, USA) with the concentration of 100 μM and incubated at 4°C for 24 h. The sample was centrifuged and the soluble portion was collected. For Aβ fibrils preparation, Aβ in DMSO at 10 mg/mL was refolded in 10 mM sodium phosphate buffer, pH 7.4. The final Aβ concentration was adjusted to 50 μM and incubated at room temperature with agitation for several days. The fibril species was monitored in the presence of 5 μM of thioflavin T (ThT) to indicate mature fibril formation. In our experiments, the differentiated N2a cells were treated with 5 μM of Aβ42 fibrils or oligomers.

We conducted the observation on Aβ42 with fluorescence microscopy and transmission electron microscopy (TEM). Fluorescein FAM-labeled Aβ42 peptides were purchased from Biopeptide (San Diego, CA). For TEM imaging, the Aβ42 samples were deposited on 400-mesh Formvar carbon-coated copper grids (EMS Electron Microscopy Sciences, Hatfield, PA, USA) for 5 min, negatively stained by 2% acetate, and rinsed by ddH_2O. The samples were examined with a Hitachi H-7000 transmission electron microscope (Chiyoda, Tokyo, Japan) with an accelerating voltage of 75 kV. Figure 3(a) and 3(b) shows the TEM micrographs of Aβ42 fibrils and oligomers, respectively. The fibrils usually formed planar aggregates, while the oligomers dispersed evenly in the field of view and therefore could hardly be identified. Figure 3(c) displays optical images of the N2a cells treated with 5 μM Aβ42 for 2.5 h. Before the optical observation, we removed the culture medium containing the Aβ42 peptides, washed the cells by PBS, and then refilled the device with the fresh medium. The fluorescence images confirmed that both the fibrils and oligomers could adhere onto the cells. Because of the larger areas of the fibril aggregations, the visibility of the fibrils was higher than that of the oligomers. Nevertheless, the actual sizes of the fibrils and oligomers were much smaller than the diffraction limit, and hence the fluorescence images could not be used as a quantitative assay of the amounts of Aβ42 peptides on the cell membranes.

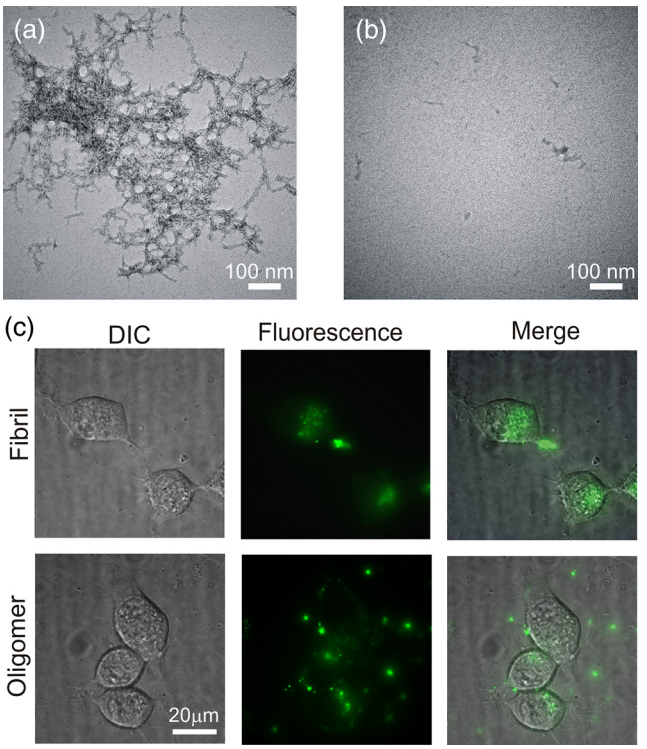

Fig. 3 (a) Transmission electron microscopy (TEM) micrograph of Amyloid-beta 42 (Aβ42) fibrils. (b) TEM micrograph of Aβ42 oligomers. (c) Optical images of N2a cells treated with the Aβ42 peptides for 2.5 h. The fluorescence signal is from the FAM fluorescein labeled on the Aβ42 peptides. DIC, differential interference contrast.

3 Results and Discussion

Figure 4 shows the membrane topography on the N2a cells obtained by NIWOP. Because the height variations on the whole cell are often larger than the NIWOP measurement dynamic range, we arbitrarily selected a 10 μm × 10 μm region at the edge of each cell, and calculated the standard deviations of the membrane height in this region as the estimation of membrane roughness. For each condition of experiment, we captured one NIWOP image per minute at the same field of view for 3 h. With both the treatments of EFs and 5 μM Aβ42 fibrils or oligomers, the cells were alive during all the experiments.

Figure 5 shows the statistics of the membrane roughness of the N2a cells under various treatments. In order to ensure that the Aβ42 peptides had sufficient time to perform their reactions on cell membranes, we compared the membrane roughness at 0.5 and 2.5 h after the treatment. In Fig. 5, we see that both the Aβ42 fibrils and oligomers reduced the membrane roughness, which could result from the increase of membrane stiffness, as reported by Lulevich et al.[8] At 0.5 h, the effect of oligomers was more significant than that of the fibrils. After 2.5 h of treatment, the fibrils reduced the membrane roughness by 18%, while the oligomers reduced the membrane roughness by 32%. The effect of Aβ42 oligomers on the roughness of N2a cell membrane was faster and stronger than that of Aβ42 fibrils. This result correlates well with the cytotoxicity of Aβ42 oligomer and Aβ42 fibrils.[8,21] These data suggest that the membrane roughness could be used as a cellular diagnostic parameter related to the effects of Aβ peptides.

We also compare the effects of dcEF and the treatment with Aβ42. The 300 mV/mm dcEF alone did not change the membrane roughness after 0.5 or 2.5 h of treatment. However, for the cells treated with Aβ42 peptides, after 2.5 h of treatment we found that the dcEF could make the roughness higher than the cells treated for 0.5 h. The effect of the dcEF was more significant on the oligomer-treated cells. The membrane roughness could be raised to the level of the control group after 2.5 h of the EF stimulation. In comparison, for the cells treated with Aβ42 fibrils, the membrane roughness was still lower than that of the control group at the 2.5th hour. This result indicates that the dcEF may counteract the change on membrane stiffness induced by Aβ42. Because the effect of Aβ42 oligomers was compensated more than that of the fibrils, we conjecture that the dcEF produces larger influences on the functions of the Aβ42 oligomers than on those of the fibrils. It has been known that Aβ oligomers can bind to cell membranes more effectively than the fibrils.[5] Liao et al. had demonstrated that negatively charged gold nanoparticles can inhibit Aβ fibril formation and reduced the cellular toxicity of Aβ oligomers.[22] Their results verified that Aβ aggregation could be affected by charged particles or molecules. We thus postulate that the dcEF effect on membrane roughness against the Aβ oligomers might also be related to the alteration of the Aβ aggregates and/or reduction of the cellular effects of Aβ peptides.

In the cell culture device shown in Fig. 1, the potential change in the cell culture region was built by the flow of Cl^-

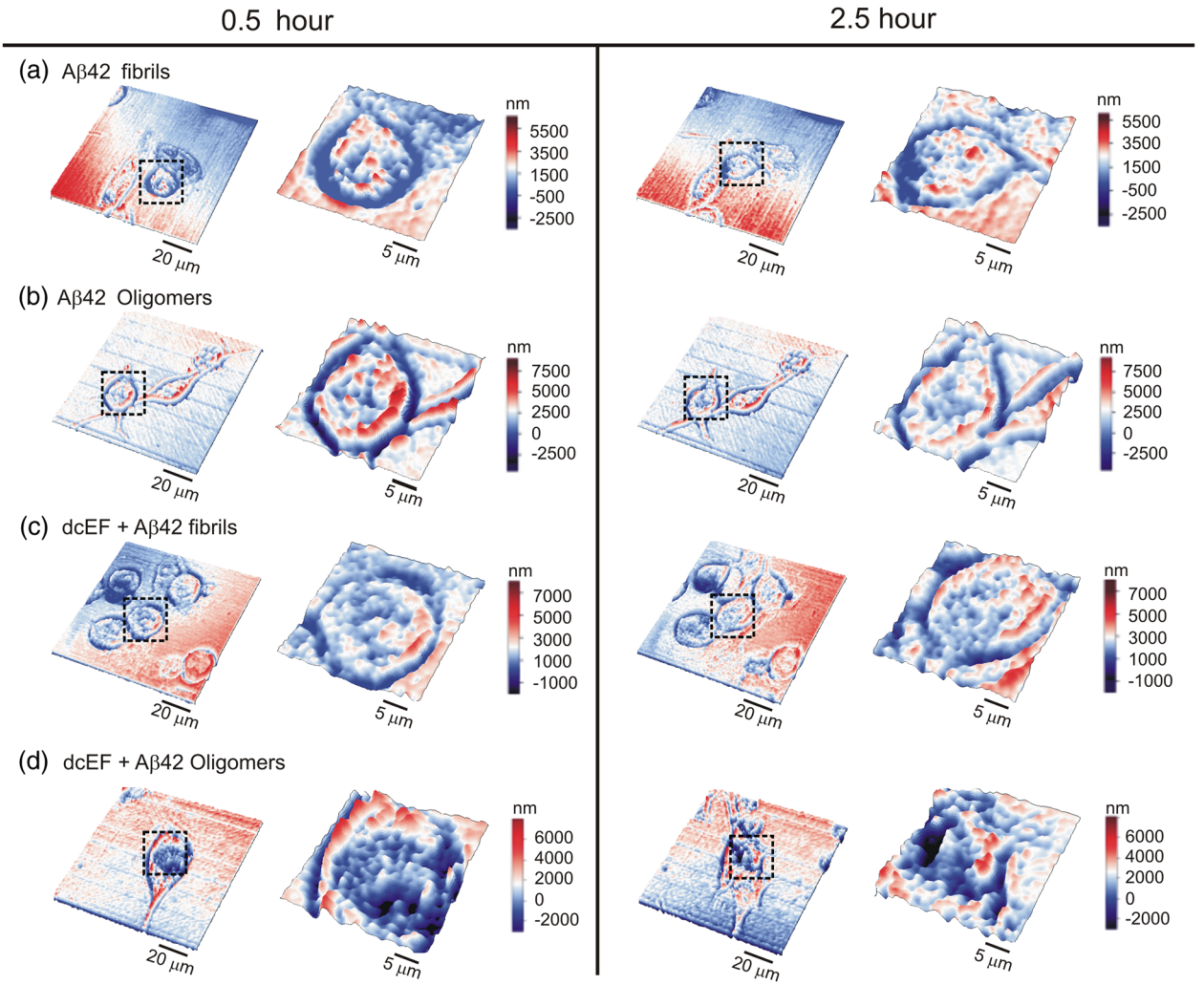

Fig. 4 The topography of Neuro-2a (N2a) cells measured by NIWOP. The left column contains the results measured after 0.5 h of treatments; while the right column shows the results after 2.5 h. In each column, the regions in the dashed boxes (30 μm × 30 μm) in the left panels are magnified in the right panels: (a) 5 μM Aβ42 fibrils treatment, (b) 5 μM Aβ42 oligomers treatment, (c) 5 μM Aβ42 fibrils and 300 mV/mm direct-current electric field (dcEF) treatment, (d) 5 μM Aβ42 oligomers and 300 mV/mm dcEF treatment.

ions. It is thus intriguing to raise the discussion about the roles of Cl^- ion channels (also called ClC channels) in such externally applied electrical stimulations. At present, the knowledge about the influence of ClC channels on Cl^- ion flux in the dcEF is still unclear. Vieira et al. have suggested that at corneal wounds an inward Cl^- ion flux produced by the ClC-2 channel may enhance wound healing,[23] probably by way of the electrotaxis effect of the nearby epithelial cells. Nevertheless, the role of the ClC-2 channel in an externally applied dcEF has not been reported yet. Moreover, to the best of our knowledge, the relation between membrane roughness and ClC channels has not been discussed in literature. In the present work, the dcEF could have triggered some cellular responses or have changed the conformation of some proteins in the ClC channel. However, these responses were not manifested in significant changes in membrane roughness, as shown in Fig. 5, where the treatment of a 300 mV/mm dcEF alone did not cause detectable changes in membrane roughness with the present NIWOP system (of which the height sensitivity is ~52 nm). In our setup, the externally applied dcEF induced a steady Cl^- flow that passed alongside the cell membrane without generating Cl^- concentration

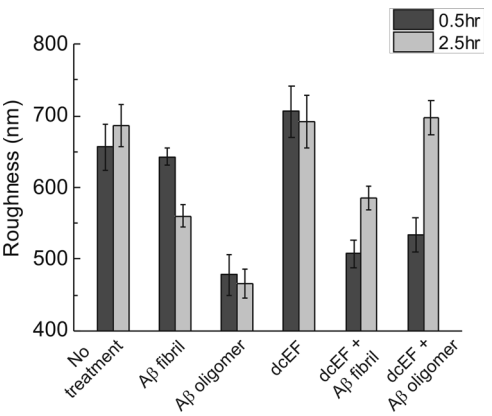

Fig. 5 Membrane roughness of N2a cells with the treatments of Aβ42 fibrils, oligomers, and a 300 mV/mm dcEF for 0.5 and 2.5 h. For each condition, >10 cells were measured in one experiment. Each experiment was repeated three times. Data show the mean ± standard error of the mean of the three experiments.

gradient across the membrane. With the present result, we could only postulate that the dcEF did impose synergic effects on membrane roughness together with Aβ42. It is also known that Aβ peptides produce cation (such as Ca^{2+}) channels on lipid bilayer membranes.[5] Therefore, the effect of external dcEFs on Aβ42 could also be related to cations. Obviously, more studies are necessary to correlate the transmembrane ion flux, Aβ42, and membrane roughness under the stimulation of dcEFs.

The measurement of the membrane fluctuations on live cells provides interesting and useful information about the cellular status. In addition to the NIWOP technique, there are more and more noncontact optical methods useful for quantifying cellular thickness or membrane topography. For example, Ding et al.[24,25] proposed a Fourier transform light scattering (FTLS) method that can reveal the dynamics of intracellular cytoskeletons in a label-free manner. The FTLS method provides reliable phase and amplitude measurements by using a common-path Mach–Zehnder interferometer setup in addition to a standard optical microscope.[24,25] Recently, Atilgan and Ovryn[26] implemented a scanning phase-shifted laser-feedback interference microscopy (psLFIM) to observe the dynamics of the retracting lamella of live cells. The psLFIM detects small variations of the refractive index of the sample in a spatially resolved way. With a well-designed algorithm, the local topography and reflectivity of the sample can be resolved from a set of interference measurements with five shifted phases.[26] Both the FTLS and the psLFIM techniques could be used as NIWOP in the present work to quantify membrane roughness. On the other hand, because the NIWOP technique relies on neither temporal nor spatial coherence to obtain the membrane topography, it provides better simplicity of setup and compatibility with existing microscopes.

4 Conclusion

In this work, we demonstrated that high-sensitivity optical profilometry was useful for the diagnosis of cellular effects of Aβ42 peptides and dcEFs. The results indicated that both Aβ42 fibrils and oligomers reduced the membrane roughness of live N2a cells. The effect of the oligomers was stronger and faster than that of the fibrils. Under Aβ42 treatment, the dcEF increased the membrane roughness in comparison with the cells treated with Aβ42 only. The efficacy of the dcEF was more obvious on the cells treated with the Aβ42 oligomer.

Interactions with Aβ peptides and plasma membranes result in alternations of biophysical as well as biochemical parameters of cell membranes. Because the NIWOP observation is label-free, the measurement on membrane roughness could be used as a convenient tool to diagnose how the chemical and physical stimulations simultaneously affect the membrane properties on live cells. This technique may be helpful for the research about evaluating the effects of various types of treatments to the neuronal cells undergoing neurodegenerative diseases.

Acknowledgments

This work was financially supported by the National Science Council of Taiwan (contract NSC 100-2112-M-001-022-MY3) and the Academia Sinica Research Program on Nanoscience and Nanotechnology.

References

1. W. Thies and L. Bleiler, "2011 Alzheimer's disease facts and figures," *Alzheimer's Dement.* **7**(2), 208–244 (2011) .
2. J. Hardy and D. J. Selkoe, "The amyloid hypothesis of Alzheimer's disease: progress and problems on the road to therapeutics," *Science* **297**(5580), 353–356 (2002).
3. Y. Verdier, M. Zarandi, and B. Penke, "Amyloid beta-peptide interactions with neuronal and glial cell plasma membrane: binding sites and implications for Alzheimer's disease," *J. Pept. Sci.* **10**(5), 229–248 (2004).
4. X. Yang, S. Askarova, and J. C. Lee, "Membrane biophysics and mechanics in Alzheimer's disease," *Mol. Neurobiol.* **41**(2–3), 138–148 (2010).
5. T. L. Williams and L. C. Serpell, "Membrane and surface interactions of Alzheimer's abeta peptide-insights into the mechanism of cytotoxicity," *FEBS J.* **278**(20), 3905–3917 (2011).
6. C. Haass and D. J. Selkoe, "Soluble protein oligomers in neurodegeneration: lessons from the Alzheimer's amyloid beta-peptide," *Nat. Rev. Mol. Cell Biol.* **8**(2), 101–112 (2007).
7. S. Lesne et al., "A specific amyloid-beta protein assembly in the brain impairs memory," *Nature* **440**(7082), 352–357 (2006).
8. V. Lulevich et al., "Single-cell mechanics provides a sensitive and quantitative means for probing amyloid-beta peptide and neuronal cell interactions," *Proc. Natl. Acad. Sci. U. S. A.* **107**(31), 13872–13877 (2010).
9. H. A. Lashuel and P. T. Lansbury Jr., "Are amyloid diseases caused by protein aggregates that mimic bacterial pore-forming toxins?" *Quart. Rev. Biophys.* **39**(2), 167–201 (2006).
10. L. Yao et al., "Small applied electric fields guide migration of hippocampal neurons," *J. Cell Physiol.* **216**(2), 527–535 (2008).
11. L. Pan and R. B. Borgens, "Strict perpendicular orientation of neural crest-derived neurons in vitro is dependent on an extracellular gradient of voltage," *J. Neurosci. Res.* **90**(7), 1335–1346 (2012).
12. M. S. Graves et al., "Electrically mediated neuronal guidance with applied alternating current electric fields," *Ann. Biomed. Eng.* **39**(6), 1759–1767 (2011).
13. A. N. Koppes, A. M. Seggio, and D. M. Thompson, "Neurite outgrowth is significantly increased by the simultaneous presentation of Schwann cells and moderate exogenous electric fields," *J. Neural Eng.* **8**(4), 046023 (2011).
14. C. Heo et al., "The control of neural cell-to-cell interactions through non-contact electrical field stimulation using graphene electrodes," *Biomaterials* **32**(1), 19–27 (2011).
15. C.-C. Wang, J.-Y. Lin, and C.-H. Lee, "Membrane ripples of a living cell measured by non-interferometric widefield optical profilometry," *Opt. Express* **13**(26), 10665–10672 (2005).
16. C.-C. Wang et al., "Dynamics of cell membranes and the underlying cytoskeletons observed by noninterferometric widefield optical profilometry and fluorescence microscopy," *Opt. Lett.* **31**(19), 2873–2875 (2006).
17. C.-H. Chen et al., "Three-dimensional characterization of active membrane waves on living cells," *Phys. Rev. Lett.* **103**(23), 238101 (2009).
18. C. D. McCaig et al., "Controlling cell behavior electrically: current views and future potential," *Physiol. Rev.* **85**(3), 943–978 (2005).
19. C.-H. Lee, H.-Y. Mong, and W.-C. Lin, "Noninterferometric wide-field optical profilometry with nanometer depth resolution," *Opt. Lett.* **27**(20), 1773–1775 (2002).
20. M. A. A. Neil, R. Juskaitis, and T. Wilson, "Method of obtaining optical sectioning by using structured light in a conventional microscope," *Opt. Lett.* **22**(24), 1905–1907 (1997).
21. K. N. Dahlgren et al., "Oligomeric and fibrillar species of amyloid-beta peptides differentially affect neuronal viability," *J. Biol. Chem.* **277**(35), 32046–32053 (2002).
22. Y.-H. Liao et al., "Negatively charged gold nanoparticles inhibit Alzheimer's amyloid-β fibrillization, induce fibril dissociation, and mitigate neurotoxicity," *Small* **8**(23), 3631–3639 (2012).
23. A. C. Vieira et al., "Ionic components of electric current at rat corneal wounds," *PLoS One* **6**(2), e17411 (2011).
24. H. Ding et al., "Fourier transform light scattering of inhomogeneous and dynamic structures," *Phys. Rev. Lett.* **101**(23), 238102 (2008).
25. H. Ding et al., "Actin-driven cell dynamics probed by Fourier transform light scattering," *Biomed. Opt. Express* **1**(1), 260–267 (2010).
26. E. Atilgan and B. Ovryn, "Reflectivity and topography of cells grown on glass-coverslips measured with phase-shifted laser feedback interference microscopy," *Biomed. Opt. Express* **2**(8), 2417–2437 (2011).